Springer

KSME

Journal of Mechanical Science and Technology 31 (3) (2017) 1203~1212
www.springerlink.com/content/1738-494x(Print)/1976-3824(Online)
DOI 10.1007/s12206-017-0219-9

Effects of feeding pipe diameter on the performance of a jet-driven Helmholtz oscillator generating pulsed waterjets †

Deng Li[1,2,3], Yong Kang[1,2,*], Xiaolong Ding[1,2], Xiaochuan Wang[1,2] and Wenchuan Liu[1,2]

[1]*School of Power and Mechanical Engineering, Wuhan University, Wuhan 430072, Hubei Province, China*
[2]*Hubei Key Laboratory of Waterjet Theory and New Technology, Wuhan University, Wuhan 430072, Hubei Province, China*
[3]*Department of Mechanical Science and Engineering, University of Illinois at Urbana-Champaign, 1206 West Green Street, Urbana, IL 61801, United States*

(Manuscript Received June 22, 2016; Revised September 22, 2016; Accepted October 19, 2016)

Abstract

Self-excited oscillation pulsed waterjet (SOPW) can take advantage of water hammer effect by generating discrete water slugs with large pressure oscillations. To further improve its efficiency, the performance of a jet-driven Helmholtz oscillator generating SOPWs was experimentally studied with feeding pipe diameter being considered. The axial pressure oscillations of the jets against the chamber length and standoff distance under four pump pressures were analyzed. It was found that feeding pipe diameter greatly affects the pressure oscillations. This dramatically depends on the pump pressure and is mainly caused by the wave and acoustic interactions in the oscillator. Feeding pipe which induces the maximum peak is the one that results in the minimum amplitude, and vice versa. Moreover, feeding pipe of diameter of 25 mm makes the amplitude fluctuate more violently at lower pump pressures. Further investigations related to the interactions of feeding pipe, hydroacoustic waves, and vorticities in shear layer should be performed.

Keywords: Self-excited oscillation; Pulsed waterjet; Feeding pipe diameter; Pressure oscillation; Helmholtz oscillator

1. Introduction

High speed waterjet is an appealing non-thermal technology that has been experiencing a rapid development during the last few decades [1]. It is presently applied in nearly all areas of modern industry, such as automotive industry, aerospace industry, construction engineering, petroleum engineering, environmental technology, chemical process engineering, and industrial maintenance [2-4]. Many researchers are focusing on improving the destructive power of high speed waterjets through creating high pressure pumps, optimizing nozzle structures, and understanding the dynamic characteristics of the jets [5-7]. It is reported that commercial high pressure systems capable of generating pressures up to 400 MPa have been available on the markets [8]. However, further enhancement of the pump pressure is still needed in order to achieve more destructive and powerful waterjets that are required in some kinds of applications. An obvious and direct consequence of further improving the pump pressure is the much higher cost to manufacture and maintain the equipment, which has been preventing the development and wide application of ultra-high pressure pumps.

An alternate approach without using ultrahigh pressure pumps is adding a certain amount of abrasive particles into the plain waterjet to create abrasive waterjet [9]. By mixing the abrasive particles with the jet in a chamber or a tube, the momentum can be transferred from the jet to the particles, which subsequently results in a great enhancement of the cutting capability and destructive power of the jet [10]. Another effective way to eliminate the need for such high pressures is to pulse the continuous waterjet into a series of discrete water slugs so as to produce pulsed waterjet. Specifically, by taking advantage of the water hammer effect, the collision of a pulsed waterjet with a solid surface is able to generate short and high pressure transients that can cause serious damage to the surface and interior of the target [11]. Moreover, pulsed waterjet is capable of generating cyclical impact forces as a consequence of the short-duration pressure pulses, which can eliminate the "cushion" effect and cause significantly greater damage to the target material compared with a plain waterjet [12]. Because of these advantages of pulsed waterjet, it has been the subject of a relative intense research effort in the Refs. [13-15].

High pressure pulsed waterjets can be generated by mechanical methods such as rotating, reciprocating, and wobbling mechanisms. For example, Dehkhoda and Hood [12, 16] developed an external-flow-interrupted pulsed waterjet device

*Corresponding author. Tel.: +86 2768774906, Fax.: +86 2768774906
E-mail address: kangyong@whu.edu.cn
† Recommended by Associate Editor Weon Gyu Shin

where the high speed rotation of a slotted disc in front of the continuous waterjet was used to generate discrete water slugs. Dehkhoda et al. [17] designed a water-filled cylindrical steel chamber with a steel piston at one end and a centrally-located nozzle mounted at the other end. Pulsed waterjet can be yielded when a hammer is used to impact the piston. However, even these devices can successfully generate pulsed waterjets with large scale of pressure and velocity oscillations, they require high levels of mechanical maintenance and have very limited lifetime and reliability in harsh working environment such as deep-hole drilling, rock cutting, and mud dredging [18].

In order to break the limitations of pulsed waterjets generated by these mechanical methods, another way of generating pulsed waterjets with the use of a Helmholtz oscillator was proposed by Morel [19]. He experimentally claimed that jet instabilities coupling with the Helmholtz resonance is able to produce very powerful chamber-pressure oscillations. And corresponding to the external-interrupted pulsed waterjet, this is defined as SOPW because it is produced by self-excited and self-sustained pressures in the oscillator without the use of any external exciting parts in the system. Then, based on some other pioneering research on self-excited oscillation and jet instabilities [19-21], several Helmholtz oscillators ("Pulser", "Laid-Back-Pulser", and "Pulser-Fed") with improved structures were designed by Johnson et al. [22]. They also carried out a series of experiments using the oscillators and concluded that the jet's performance can be doubled with respect to the erosivity, as compared to a steady jet having an equivalent mean pressure drop.

Due to the significant advantages of SOPW over a mechanically generated pulsed waterjet, it has been studied extensively as a fundamental problem in turbulence and as a new technology in engineering applications. In more specific terms, Hasan and Hussain [23] explored the characteristics of a self-excited axisymmetric jet experimentally and found that self-excitation produces a large increase in the fluctuation intensity in the near field of the jet when compared with a corresponding unexcited jet. Arthurs and Ziada [24] experimentally examined the acoustic tone generation of a high speed self-excited jet over a wide range of jet velocities. They concluded that the acoustic tones are generated by both symmetric and anti-symmetric jet instabilities. Moreover, Li et al. [25, 26] studied the effects of nozzle inner surface roughness on the axial pressure oscillation and cavitating erosion characteristics of self-resonating cavitating pulsed waterjets, which have the same generation mechanism with SOPW. In addition, Li et al. [27] also found that area discontinuity at nozzle inlet greatly affects the characteristics of self-resonating cavitating pulsed waterjet, which provides a novel way to improve the performance of the jet. Furthermore, Fang et al. [28] performed a numerical investigation on the influence of collapse wall on the pressure oscillations of SOPW, aiming at improving the performance of the jet through optimizing the nozzle structure. They demonstrated that the upper wall plays a more important role than the lower wall in affecting the pressure oscillations.

As for the applications of SOPWs, Wang et al. [29] developed a modulating tool with a suction-type Helmholtz oscillation built-in, aiming at further improving the rate of penetration. And they claimed that this tool is more reliable and durable because it has simpler structure and no moving parts. On the other hand, Yang et al. [30] investigated the dynamic characteristics of SOPW discharging from a Helmholtz oscillator used as the breaking and losing device for air-lift pump. They pointed out that SOPW not only effectively breaks the hard rock but also produces fluctuating uplift forces acting on the sand particles. Moreover, by applying SOPW in mine gas extraction, Li et al. [31] found the gas absorption rate can be decreased by 30 %~40 % and the penetrability coefficient can be increased 100 times.

In the considerable number of papers published on SOPW, however, most of them are dealing with the generation mechanisms, structure optimization, or engineering applications. To the best of our knowledge, nearly no one has ever considered feeding pipe diameter as an important factor affecting the characteristics of SOPW. But feeding pipe diameter should deserve some attention when wave propagation and self-excitation are taken into account. To be more specific, Rienstra [32] concluded from an analysis of acoustic wave-pipe-jet flow interaction that the velocity and pressure fields inside the pipe and the pressure far field are related to the pipe diameter, indicating feeding pipe diameter could affect the performance of SOPW. Herrmann et al. [33] pointed out that the wave damping characteristics are determined by pipe diameter, suggesting that feeding pipe diameter is related to the performance of the jet. Since SOPW is resulted from a standing wave generated in the oscillator, this suggests that feeding pipe diameter is related to the performance of the jet. Moreover, in one of the pioneering efforts on a jet-driven oscillating pulsed jet, Morel [19] has particularly pointed out that some attention should be given to the feeding pipe geometry, because it could have great effects on the oscillation characteristics of the jet. To be honest, in one of our previous experiments on SOPW, it has been stumbled upon that the erosion capability of the jet was dramatically changed after the feeding pipe had been replaced by another one with a different diameter, which actually most promoted this study.

The objective of this study is to improve the performance of Helmholtz oscillator for producing high speed waterjets with stronger self-excited and self-sustained pressure fluctuations. To reach this goal, effects of feeding pipe diameter were experimentally investigated as an attempt, with a focus on the axial pressure fluctuation peak and amplitude.

2. Working principles of a Helmholtz oscillator

As shown in Fig. 1, a Helmholtz oscillator is constructed of a cylindrical shell and two circular end plates called upstream nozzle and downstream nozzle respectively. The cavity formed by these three parts is called oscillation chamber. And

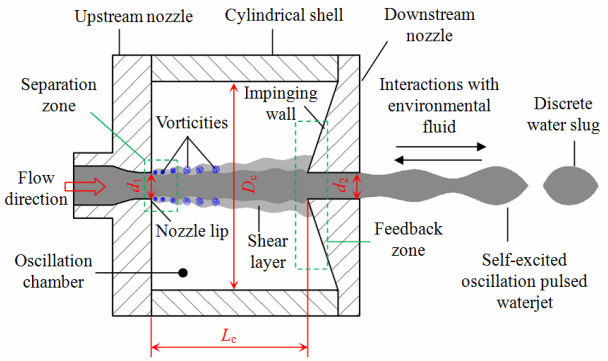

Fig. 1. Working principles of a jet-driven Helmholtz oscillator.

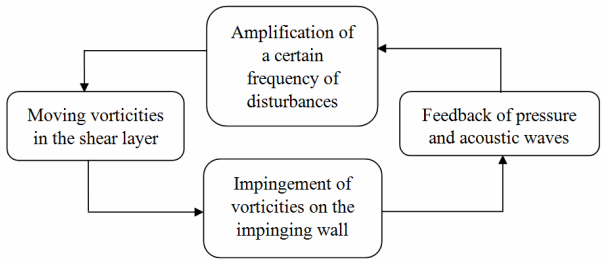

Fig. 2. Closed loop of self-excited and self-sustained oscillation.

each end plate has at its center an orifice coaxial with the axis of the cylindrical shell. It should be pointed out that the inner side of the downstream nozzle is not flat, but is a frustum with a certain angle and called impinging wall.

When a high speed jet emerges into the oscillation chamber, shear layer will be formed in the separation zone because of the sudden changes of pressure and stress distributions in the flow. And according to the boundary/shear layer and fluid mechanics theory, disturbances will be formed by the nozzle lip-jet interactions. Furthermore, the combination of these disturbances with the Kelvin-Helmholtz instability of the jet is able to result in vorticities formed in the shear layer. The vorticities and shear layer move downwards and then impinge on the impinging wall, yielding pressure and acoustic waves of different frequencies at the feedback zone. Then, these pressure and acoustic waves propagate upwards at the local sound speed. A specific frequency of wave can significantly amplify the same frequency of disturbances at the separation zone, leading to much more and stronger vorticities generated at the separation zone. The enhanced vorticities will certainly cause stronger pressure and acoustic waves generated and reflected at the feedback zone. Thus, a closed loop of this self-excited and self-sustained oscillation is shaped and shown in Fig. 2.

If the wave frequency, f_w, matches the fundamental frequency of the Helmholtz oscillator, f_0, and also the jet structuring frequency, f_s, peak resonance will be formed in the oscillation chamber, which will subsequently cause great pressure oscillations that can make the jet more unstable. On the other hand, after the jet discharges from the downstream nozzle, its interactions with the environmental fluid will intensify the instability of the jet. Under these conditions, the continuous jet will be pulsed into discrete water slugs, and a SOPW is finally generated. As the match of the three frequencies is particularly important in designing an effective Helmholtz oscillator, the mathematic expressions of the frequencies are presented below.

The wave frequency can be defined as [34]:

$$f_w = \frac{N}{L_c\left(\frac{1}{a_+}+\frac{1}{a_-}\right)} \tag{1}$$

where N is model number; L_c is the length of the oscillation chamber; a_+ and a_- are the velocities of waves travelling downwards and upwards respectively, and can be written as:

$$\begin{aligned} a_+ &= a + U \\ a_- &= a - U \end{aligned} \tag{2}$$

where a is local sound speed; and U is jet velocity.

As for the fundamental frequency of the Helmholtz oscillator, it can be expressed as [35]:

$$f_0 = \frac{a}{2\pi}\sqrt{\frac{A_0}{V\left(l_0+\beta d_1\right)}} \tag{3}$$

where A_0 is the cross area of nozzle inlet; l_0 is the length of nozzle inlet; V is the volume of the oscillation chamber; β is a correction factor of 0.6; and d_1 is the inlet diameter.

In terms of the jet structuring frequency, it is obvious that:

$$f_s = \frac{S_t U}{d_1} \tag{4}$$

where S_t is Strouhal number, and is usually given a value of 0.3, according to the previous investigations [19-22, 25-28].

More detailed information on jet-driven Helmholtz oscillator for generating SOPWs can be achieved in Refs. [19, 22, 28, 29, 31, 36]. However, it should be noted that the detailed design of a jet-driven Helmholtz oscillator for successfully generating SOPWs is quite complex, and currently the absence of a theoretical and quantitative explanation of the mechanism makes experimental investigation the main method in the study of SOPWs [22, 26].

3. Experimental system and procedures

In terms of SOPWs, the intensity of pressure oscillation is an important criterion to evaluate the effectiveness of a SOPW. Thus, effects of feeding pipe diameter on the performance of the jet-driven Helmholtz oscillator were evaluated by the pressure characteristics of the jets under different conditions, which were different pump pressures, chamber lengths, and standoff distances.

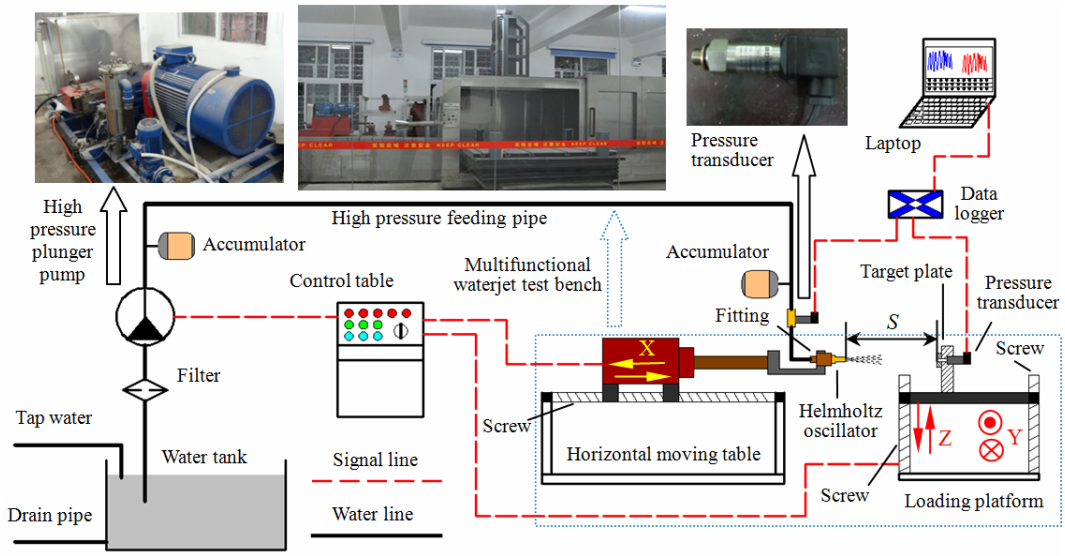

Fig. 3. Experimental setup for measuring the axial pressure.

3.1 Experimental setup and procedures

Fig. 3 is a schematic diagram of the experimental setup for measuring the axial pressures of SOPWs discharging from the Helmholtz oscillator. The experiment was performed on a multifunctional waterjet test bench developed by our research team and had been used in some of our previous research [25-27]. High pressure waterjets were provided by a plunger pump whose maximum pressure and flow rate were 60 MPa and 120 L/min, respectively. By using the control table, pump pressure could be continuously regulated by changing the frequency of the motor powering for the pump. The experiment was performed under four pump pressures (P_u), which were 10 MPa, 15 MPa, 20 MPa and 25 MPa.

As is shown in Fig. 3, the Helmholtz oscillator installed on the walking device could be given a motion in the X direction, while a target plate fixed on the loading platform could be given motions in the Y and Z directions. The target plate had at its center a hole with a diameter of 1 mm, which was smaller than that of the jet. Moreover, a pressure transducer (Model: BD Sensors DMP333) was installed on the target plate, communicating with the hole. By adjusting the location of the target plate, the axis of the nozzle could be made coaxial with that of the hole on the target plate. As a consequence, SOPWs could impact perpendicularly on the plate in each test, which then ensured the reliability of the results. For better analyzing the effects of feeding pipe diameter, another pressure transducer was installed in the flow path to get the pressure (inlet pressure P_i) of the flow just before it entered into the Helmholtz oscillator.

Standoff distance, S, which was defined as the distance from the nozzle exit to the plate surface, could be continuously changed by horizontally moving the oscillator. And in the experiment, standoff distance was changed from 10 mm to 100 mm with an interval of 10 mm.

The pressure oscillation amplitude was defined as the difference of the maximum pressure and the minimum pressure appeared in the period of each test, and could be expressed as:

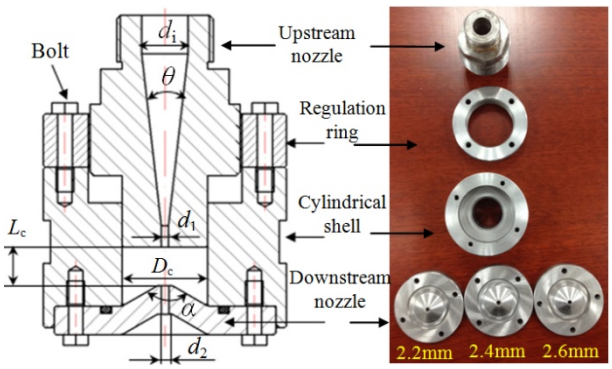

Fig. 4. Profile and photo of the testing Helmholtz oscillator.

$$P_a = P_{max} - P_{min} \tag{5}$$

where P_a is the pressure oscillation amplitude; P_{max} is the pressure oscillation peak; and P_{min} is the minimum pressure. Both P_{max} and P_{min} could be read directly from the laptop connected with the data logger.

3.2 Helmholtz oscillator and feeding pipes

Fig. 4 shows the structure and picture of the Helmholtz oscillator used in the experiment. According to the previous researchs [18, 22, 34], the ratios of the chamber length and downstream diameter to the upstream diameter are rather important to the performance of Helmholtz oscillator. Therefore, effects of feeding pipe diameter were also studied under different ratios in the following section.

As is illustrated in Fig. 4, a regulation ring was applied to ensure the continuous change of chamber length, L_c, from 0

Table 1. Specifications of the feeding pipes.

Pipe size/mm	Inside diameter/mm	Outside diameter/mm	Working pressure/bar	Burst pressure/bar
6	6±0.5	18±0.8	600	1800
13	13±0.5	24±0.8	420	1600
25	25±0.5	42±1	380	1520

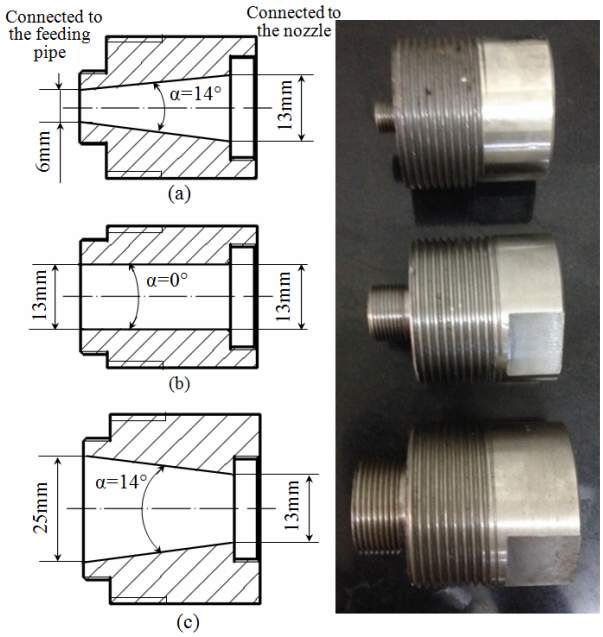

Fig. 5. Profiles and photos of the three fittings.

mm to 40 mm. For the upstream nozzle, the inlet diameter was d_i = 13 mm, the convergence angle was θ = 14°, and the upstream diameter was d_1 = 2 mm. The diameter of the chamber was D_c = 24 mm and the taper angle of the impinging wall was α = 120°. And three downstream nozzles with diameters of d_2 = 2.2 mm, 2.4 mm and 2.6 mm were employed in the experiment. All these geometrical parameters were determined according to the previous investigations [18, 22, 34].

Three feeding pipes with inner diameters of 6 mm, 13 mm and 25 mm were used in the experiment. They had the same length of 10 m and all came from the same manufacturer. The main specifications of the three feeding pipes are shown in Table 1.

3.3 Disturbance elimination

From Sec. 2, it is known that SOPWs origin from an effective amplification of the initial disturbances generated in the free shear layer. In order to eliminate other disturbances that could affect the results, two bladder accumulators were used to minimize the pressure or flow rate fluctuations of the pump. As is depicted in Fig. 3, one accumulator was positioned closely to the pump and the other was situated immediately next to the Helmholtz oscillator.

Since the difference between feeding pipe diameter and inlet diameter could cause disturbances at the oscillator inlet, three fittings were used to make the flow enter into the oscillator steadily. The flow passages in fittings (a) and (c) changed smoothly from one end to the other end with an angle of 14°, as shown in Fig. 5. As a result, the unwanted disturbances could be obviously eliminated and feeding pipe diameter was made the only variable in each test.

Table 2. Inlet pressure corresponding to each pump pressure.

Feeding pipe diameter D_f/mm	Pump pressure P_u/MPa			
	10	15	20	25
	Inlet pressure P_i/MPa			
6	9.29	14.07	18.96	23.81
13	9.91	14.82	19.54	24.80
25	9.96	14.95	19.94	24.93

3.4 Experimental uncertainties

As pressure oscillation peak and amplitude were used to evaluate the effects of feeding pipe diameter, the main experimental uncertainty came from the accuracy of pressure transducer used to measure the axial pressure of the jets. And this pressure transducers had been calibrated by the manufacture with an accuracy of ±0.2 %FS. Other experimental uncertainties, even not so important, included the accuracies of the pressures transducers used to obtain the pump and inlet pressures, which were both ±0.5 %FS. In addition, the accuracy class of the data logger was 0.05, and the linearity error and zero drift were ±0.02 %FS and 0.02 %/10K, respectively.

4. Results and discussion

It should be clear that the most obvious effect of feeding pipe diameter is the different linear pressure losses in the pipeline. In order to give a better investigation on other more important effects of feeding pipe diameter on the performance of the oscillator, this effect was isolated by comparing the average inlet pressures under each condition, as shown in Table 2.

It is evident from Table 2 that the pressure loss in the pipeline increases with decreasing feeding pipe diameter under each pump pressure. And at higher pump pressures, the pressure loss for each feeding pipe diameter is also greater. However, it should be noted that the differences caused by feeding pipe diameter are not so important. Because the largest difference of pressure loss is only 1.12 MPa, which appears between D_f = 6 mm and D_f = 25 mm at pump pressure of 25 MPa.

4.1 Pressure oscillation peak against chamber length

Our preliminary tests have shown that the most appropriate ratios of downstream nozzle diameter to upstream nozzle diameter in this experiment are 1.1, 1.1, 1.2 and 1.2, corresponding to pump pressures of 10 MPa, 15 MPa, 20 MPa and

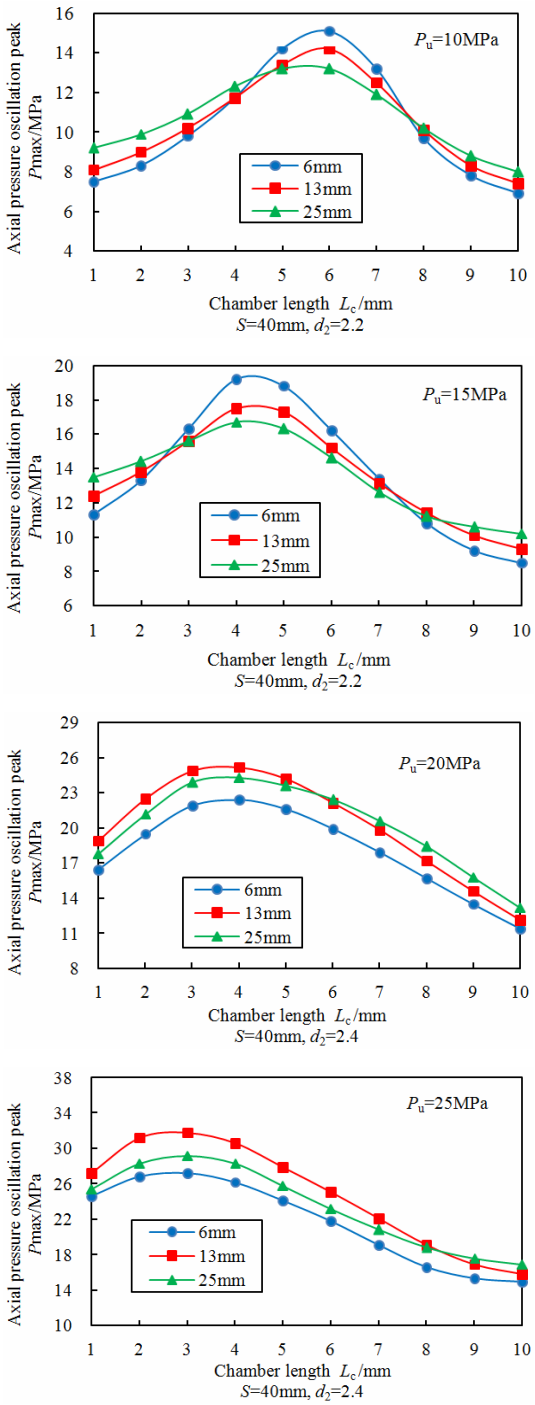

Fig. 6. Axial pressure oscillation as a function of chamber length at different pump pressures.

25 MPa, respectively [37]. As Morel [19] has pointed out that the interactions between feeding pipe and the oscillator volume is of great importance, here the axial pressure oscillation peaks of the jets against chamber length under each pump pressure are plotted in Fig. 6.

The chamber length for achieving the greatest axial pressure oscillation peak is defined as optimal length, which is decreasing with the increase of pump pressure. This is due to the fact that the jet velocity is larger at higher pump pressures, resulting in the increase of the structuring frequency, shown in Eq. (4). As a consequence, the fundamental frequency of the Helmholtz oscillator should increase so as to match the structuring frequency and cause resonance. According to Eq. (3), it is clear that decreasing the volume of the chamber can increase the fundamental frequency. Since the chamber diameter is fixed, the decrease of the volume can only be achieved by decreasing the chamber length. In more specific terms, the optimum chamber lengths are 6 mm, 4 mm, 3.5 mm and 3 mm, corresponding to pump pressures of 10 MPa, 15 MPa, 20 MPa and 25 MPa, respectively. And it is evident from the figure that, feeding pipe diameter nearly has no influence on this phenomenon. In other words, feeding pipe diameter almost has no ability to change the oscillating frequency of SOPWs, which is in good agreement with our previous research on the characteristics of self-resonating pulsed waterjets influenced by feeding pipe diameter [38].

However, feeding pipe diameter can greatly affect the value of the axial pressure oscillation peak, especially near the optimal chamber lengths. More specifically, feeding pipe with diameter of 6 mm can make the pressure oscillation peak reach 15.13 MPa and 19.21 MPa, respectively, corresponding to chamber lengths of 6 mm and 4 mm and pump pressures of 10 MPa and 15 MPa; while at pump pressures of 20 MPa and 25 MPa, feeding pipe with diameter of 13 mm takes its place to cause the greatest pressure oscillation peaks of 24.92 MPa and 31.81 MPa, respectively. As is shown in Fig. 6, it is also found that the same feeding pipe affects the pressure oscillation peak against chamber length differently, depending on the pump pressure. For example, at pump pressure of 10 MPa, even feeding pipe of diameter of 6 mm causes the greatest peaks at chamber length between 5 mm and 7 mm, it also makes the smallest peaks at all the other chamber lengths. However, this feeding pipe is always the one that leads to the lowest peaks at pump pressure of 25 MPa.

These tests also provide the optimum chamber lengths corresponding to each pump pressure for conducting the following experiment on the pressure oscillation peak and amplitude with varying standoff distance, since the optimum structure of Helmholtz oscillator should be applied in applications.

4.2 Pressure oscillation peak against standoff distance

Fig. 7 shows the pressure oscillation peaks at various standoff distances and the four pump pressures. It is of great interest to observe that, the shape of each curve is rather similar with that of the corresponding curve in Fig. 6. Each curve first goes up and then goes down with a crest at a certain standoff distance, called optimal standoff distance. The optimal standoff distance mainly depends on the pump pressure, meaning feeding pipe diameter can hardly affect it. And the optimal standoff distances are about 45 mm (S_{01}), 40 mm (S_{02}), 35 mm (S_{03}) and 30 mm (S_{04}), corresponding to pump pressures of 10 MPa, 15 MPa, 20 MPa and 25 MPa, respectively.

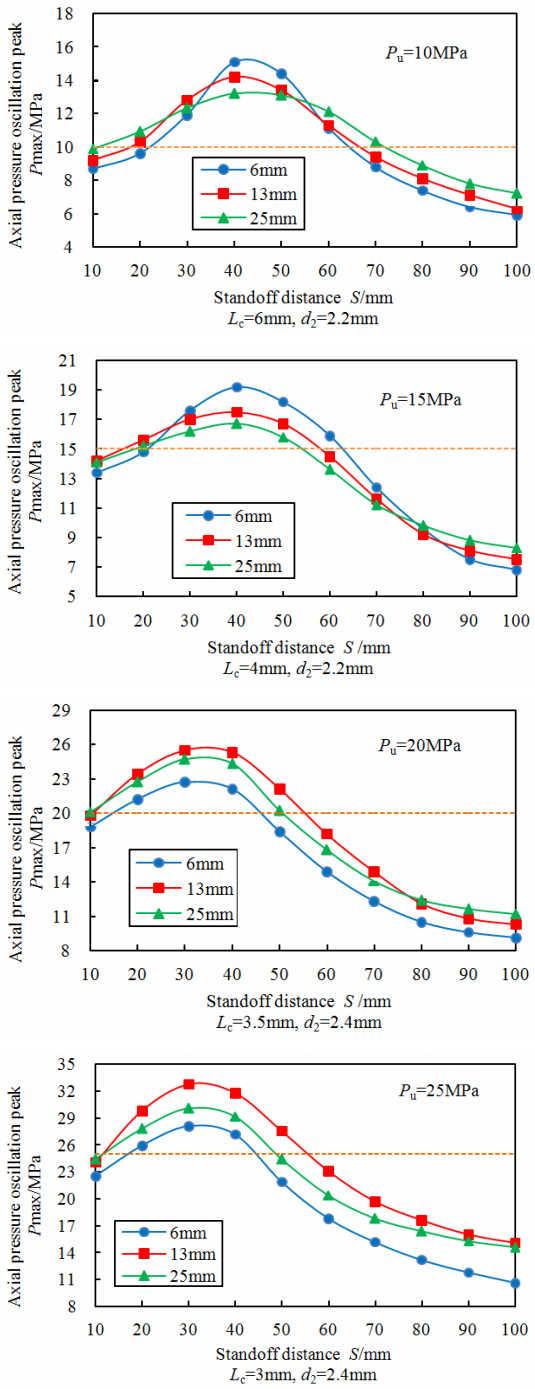

Fig. 7. Axial pressure oscillation peak as a function of standoff distance at different pump pressures.

Furthermore, if the linear pressure loss in the pipeline is taken into account, a relation between the four optimal standoff distances could be achieved, which is:

$$S_{o1} \approx \sqrt{3/2}S_{o2} \approx \sqrt{2}S_{o3} \approx \sqrt{5/2}S_{o4} . \quad (6)$$

In order to give an explanation on this relationship, here we give a preliminary analysis with respect to the jet instability wave which is an important and necessary requirement for generating SOPWs. To obtain the jet velocity, Bernoulli equation is applied:

$$Z_1 + \frac{P}{\rho g} = Z_2 + \frac{\gamma u^2}{2g} + h_l + h_j . \quad (7)$$

Here, $Z_1 = Z_2$, and ignore linear loss h_l and local loss h_j, we can get:

$$u_1 = \sqrt{2/3}u_2 = \sqrt{1/2}u_3 = \sqrt{2/5}u_4 . \quad (8)$$

Combine Eqs. (4) and (8), the relation of jet structuring frequencies under the four pump pressures can be obtained:

$$f_{v1} = \sqrt{2/3}f_{v2} = \sqrt{1/2}f_{v3} = \sqrt{2/5}f_{v4} . \quad (9)$$

For the instability wavelength, there is $\lambda = c/f$. Hence, the relation between the wavelengths at different pump pressures can be obtained as follows:

$$\lambda_1 \approx \sqrt{3/2}\lambda_2 \approx \sqrt{2}\lambda_3 \approx \sqrt{5/2}\lambda_4 \approx \sqrt{3}\lambda_5 . \quad (10)$$

Therefore, it can be concluded from Fig. 7 that the optimal standoff distance has a proportional relation with jet instability wavelength, which is regardless of feeding pipe diameter.

Moreover, it is even more amazing that the relations and trends of the curves under each pump pressure are almost the same with those in Fig. 6, suggesting that the effects of feeding pipe diameter are very similar under these conditions. However, it should be emphasized that the reasons behind Figs. 6 and 7 are completely different. Specifically, the phenomenon that the pressure oscillation peak first increases and then decreases with increasing chamber length in Fig. 6 is caused by the need of a match of the jet structuring frequency and the fundamental frequency of the Helmholtz oscillator. Only the optimal chamber length can result in the resonance in the oscillator and the strongest pressure oscillations [18, 19, 37]. On the other hand, the existence of an optimum standoff distance at each pump pressure in Fig. 7 is mainly attributed to the fact that the pressure or flow rate of the jet is most discrete at a certain standoff distance. Since SOPW is derived from jet instabilities, a certain time is needed to allow the instability wave and aerodynamic interactions to become the strongest [21, 22].

Another interesting phenomenon can be observed in Fig. 7 is that the range of effective standoff distance where the peak pressure is larger than the corresponding pump pressure (the rage where curves are above the orange dash line) is dramatically affected by feeding pipe diameter. At pump pressures of 10 MPa and 15 MPa, feeding pipe diameter that results in both the greatest pressure oscillation peak and the range of effective standoff distance cannot be achieved; while at pump pressures of 20 MPa and 25 MPa, feeding pipe with a diameter of

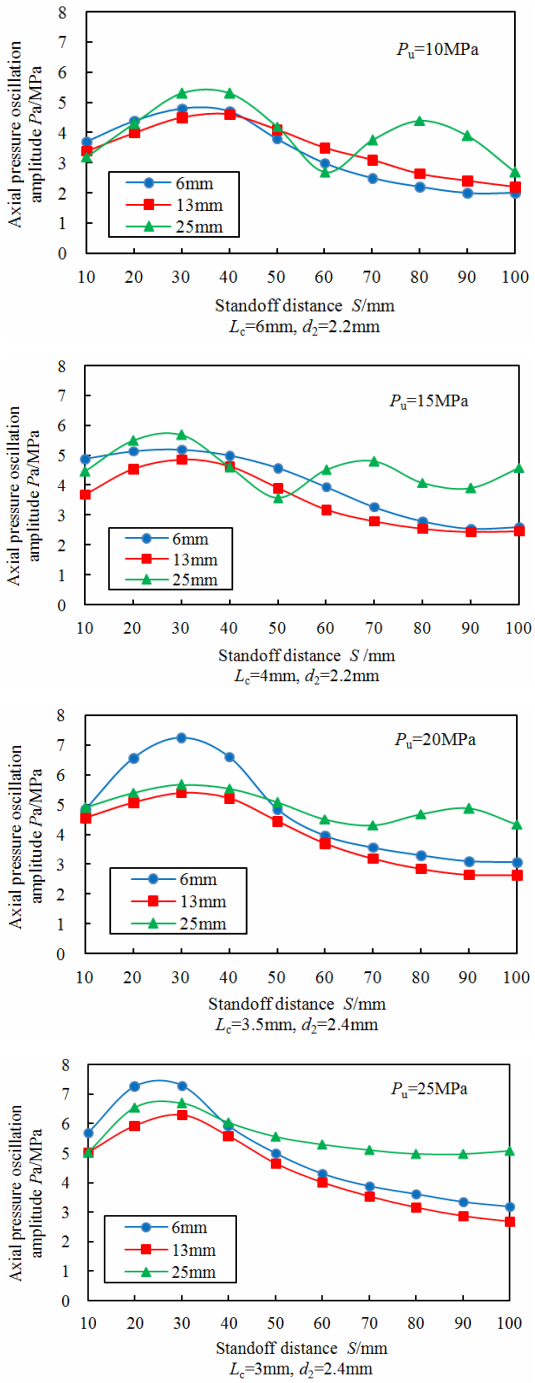

Fig. 8. Axial pressure oscillation amplitude as a function of standoff distance at different pump pressures.

13 mm is the most appropriate one.

4.3 Pressure oscillation amplitude against standoff distance

Fig. 8 illustrates the pressure oscillation amplitudes at various standoff distances and pump pressures. It is obvious from the figure that feeding pipe diameter has significant effects on the pressure oscillation amplitudes of SOPWs, and these effects also greatly depend on the pump pressure.

As depicted in Fig. 8, the pressure oscillation amplitudes are larger at higher pump pressures, meaning the oscillations are stronger and the jets are more unstable. And this seems to be a common feature of SOPWs, which is independent of feeding pipe diameter. Moreover, the blue and red curves have almost the same trend with an increase at first and a decrease followed under all the four pump pressures, indicating that feeding pipes of diameters of 6 mm and 13 mm affect the pressure oscillation amplitude in the same way. The crests of these two curves under each pump pressure are the same, which are about 40 mm, 35 mm, 30 mm and 25 mm, respectively, corresponding to pump pressures of 10 MPa, 15 MPa, 20 MPa and 25 MPa. Compared with the optimal standoff distances in Fig. 7, these four standoff distances for achieving the largest pressure oscillation amplitudes are 5 mm smaller than the corresponding ones. In other words, the standoff distances where the maximum pressure oscillation peak and amplitude appear are kind of inconsistent. This could be attributed to the wave and acoustic interactions between feeding pipe and the Helmholtz oscillator; however, current related literature is far from enough to clarify this phenomenon.

It should be evident from Fig. 8 that the pressure oscillation amplitude affected by feeding pipe of diameter of 25 mm is dramatically different from that influenced by the other two feeding pipes. In more specific terms, the pressure oscillation amplitude fluctuates with increasing standoff distance rather than simply goes up and down. Furthermore, the intensity of fluctuation reduces with the increase of pump pressure, especially at larger standoff distances. And at pump pressure of 25 MPa and standoff distances exceeding 50 mm, the pressure oscillation amplitude affected by feeding pipe diameter of 25 mm decreases very gradually and nearly keeps stable with a value of about 5 MPa.

It is of great interest to notice that feeding pipe, which maximally raises the pressure oscillation peak around the optimal standoff distance, is the one that results in the smallest amplitude around the corresponding standoff distance, and vice versa. For example, at pump pressures of 10 MPa and 15 MPa, feeding pipe diameter of 6 mm can cause the largest pressure oscillation peak, while it leads to the smallest pressure oscillation amplitude. Further investigations should be conducted to give a good explanation on these phenomena.

5. Conclusions

(1) Feeding pipe diameter directly affects the linear pressure loss in the pipeline, which is negligible when compared with the effects on the axial pressure oscillations of SOPWs. These effects are probably resulted from the wave and acoustic interactions of feeding pipe and the Helmholtz oscillator.

(2) The optimum chamber length decreases with increasing pump pressure regardless of feeding pipe diameter. But feeding pipe diameter greatly can affect the value of the axial pressure oscillation peak, especially at chamber lengths near the

optimum.

(3) The effects of feeding pipe diameter on the pressure oscillation peak against chamber length and standoff distance are almost the same, but the reasons of these two phenomena are different.

(4) In terms of the pressure oscillation amplitude, feeding pipe of diameter of 25 mm makes it fluctuate against standoff distance especially at lower pump pressures, which is dramatically different from that caused by the other two feeding pipes.

(5) Further experimental and theoretical research should be performed to better explain the effects of feeding pipe diameter, aiming at improving the performance of the jet-driven Helmholtz oscillator.

Acknowledgment

This research is financially supported by the National Key Basic Research Program of China (No. 2014CB239203), the National Natural Science Foundation of China (No. 51474158) and the China Scholarship Council (No. 201406270047).

References

[1] M. G Mostofa, K. Y. Kil and A. J. Hwan, Computational fluid analysis of abrasive waterjet cutting head, *Journal of Mechanical Science and Technology*, 24 (1) (2010) 249-252.

[2] X. Liu, S. Liu and H. Ji, Mechanism of rock breaking by pick assisted with water jet of different modes, *Journal of Mechanical Science and Technology*, 29 (12) (2015) 5359-5368.

[3] A. Guha, R. M. Barron and R. Balachandar, An experimental and numerical study of water jet cleaning process, *Journal of Materials Processing Technology*, 211 (4) (2011) 610-618.

[4] M. Santhanakumar, R. Adalarasan and M. Rajmohan, Parameter design for cut surface characteristics in abrasive waterjet cutting of Al/SiC/Al2O3 composite using grey theory based RSM, *Journal of Mechanical Science and Technology*, 30 (1) (2016) 371-379.

[5] V. N. Lad and Z. V. P. Murthy, Effects of the geometric orientations of the nozzle exit on the breakup of free liquid jet, *Journal of Mechanical Science and Technology*, 30 (4) (2016) 1625-1630.

[6] C. Y. Hsu, C. C. Liang, T. L. Teng and A. T. Nguyen, A numerical study on high-speed water jet impact, *Ocean Engineering*, 72 (2013) 98-106.

[7] M. Monno and C. Ravasio, *The effect of pressure on the surfaces generated by waterjet: preliminary analysis*, Springer Vienna (2005).

[8] J. Foldyna, L. Sitek, B. Švehla and Š. Švehla, Utilization of ultrasound to enhance high-speed water jet effects, *Ultrasonics Sonochemistry*, 11 (3) (2004) 131-137.

[9] G. Cosansu and C. Cogun, An investigation on use of colemanite powder as abrasive in abrasive waterjet cutting (AWJC), *Journal of Mechanical Science and Technology*, 26 (8) (2012) 2371-2380.

[10] D. H. Ahmed, J. Naser and R. T. Deam, Particles impact characteristics on cutting surface during the abrasive water jet machining: Numerical study, *Journal of Materials Processing Technology*, 232 (2016) 116-130.

[11] J. Foldyna, L. Sitek, J. Ščučka, P. Martinec, J. Valíček and K. Páleníková, Effects of pulsating water jet impact on aluminium surface, *Journal of Materials Processing Technology,* 209 (20) (2009) 6174-6180.

[12] S. Dehkhoda and H. Michael, An experimental study of surface and sub-surface damage in pulsed water-jet breakage of rocks, *International Journal of Rock Mechanics and Mining Sciences*, 63 (2013) 138-147.

[13] Y. Liu, J. Wei, T. Ren and Z. Lu, Experimental study of flow field structure of interrupted pulsed water jet and breakage of hard rock, *International Journal of Rock Mechanics and Mining Sciences*, 78 (2015) 253-261.

[14] P. N. Karpov, A. D. Nazarov, A. F. Serov and V. I. Terekhov, Evaporative cooling by a pulsed jet spray of binary ethanol-water mixture, *Technical Physics Letters*, 41 (7) (2015) 668-671.

[15] I. Lee, Y. Kang and J. Koo, Mixing characteristics of pulsed air-assist liquid jet into an internal subsonic cross-flow, *Journal of Thermal Science*, 19 (2) (2010) 136-140.

[16] S. Dehkhoda and M. Hood, The internal failure of rock samples subjected to pulsed water jet impacts, *International Journal of Rock Mechanics and Mining Sciences*, 66 (2014) 91-96.

[17] S. Dehkhoda, M. Hood, H. Alehossein and D. Buttsworth, Analytical and experimental study of pressure dynamics in a pulsed water jet device, *Flow, Turbulence and Combustion*, 89 (1) (2012) 97-119.

[18] D. Hu, X. H. Li, C. L. Tang and Y. Kang, Analytical and experimental investigations of the pulsed air–water jet, *Journal of Fluids and Structures*, 54 (2015) 88-102.

[19] T. Morel, Experimental study of a jet-driven Helmholtz oscillator, *Journal of Fluids Engineering*, 101 (3) (1979) 383-390.

[20] S. C. Crow and F. H. Champagne, Orderly structure in jet turbulence, *Journal of Fluid Mechanics*, 48 (3) (1971) 547-591.

[21] D. Rockwell and E. Naudascher, Self-sustained oscillations of impinging free shear layers, *Annual Review of Fluid Mechanics*, 11 (1) (1979) 67-94.

[22] V. E. Johnson, W. T. Lindenmuth, A. F. Conn and G. S. Frederick, Feasibility study of tuned-resonator, pulsating cavitating water jet for deep-hole drilling, *No. SAND-81-7126*, Sandia National Labs., Albuquerque, NM (USA); Hydronautics, Inc., Laurel, MD, USA (1981).

[23] M. A. Z. Hasan and A. K. M. F. Hussain, The self-excited axisymmetric jet, *Journal of Fluid Mechanics*, 115 (1982) 59-89.

[24] D. Arthurs and S. Ziada, Self-excited oscillations of a high-speed impinging planar jet, *Journal of Fluids and Structures*, 34 (2012) 236-258.

[25] D. Li, Y. Kang, X. Wang, X. Ding and Z. Fang, Effects of nozzle inner surface roughness on the cavitation erosion characteristics of high speed submerged jets, *Experimental Thermal and Fluid Science*, 74 (2016) 444-452.

[26] D. Li, X. Li, Y. Kang, X. Wang, X. Long and S. Wu, Experimental investigation on the influence of internal surface roughness of organ-pipe nozzle on the characteristics of high speed jet, *Journal of Mechanical Engineering*, 51 (17) (2015) 169-176 (in Chinese).

[27] D. Li, Y. Kang, X. Ding, X. Wang and Z. Fang, Effects of Area Discontinuity at Nozzle Inlet on the Characteristics of Self-resonating Cavitating Waterjet, *Chinese Journal of Mechanical Engineering* (2016) 1-12.

[28] Z. Fang, Y. Kang, X. Yang, B. Yuan and D. Li, The influence of collapse wall on self-excited oscillation pulsed jet nozzle performance, *IOP Conference Series: Earth and Environmental Science*, 15 (5) 052022, IOP Publishing (2012).

[29] P. Wang, H. Ni, R. Wang and Z. Li, Modulating downhole cuttings via a pulsed jet for efficient drilling-tool development and field testing, *Journal of Natural Gas Science and Engineering*, 27 (2015) 1287-1295.

[30] L. Yang, S. P. Cai and C. L Tang, Study on improving performance of airlift device by self-excited oscillation pulsed jet used in mining under water, *Journal of Coal Science and Engineering (China)*, 14 (2008) 683-685.

[31] X. H. Li, D. P. Zhou, Y. Y. Lu, Y. Kang, Y. Zhao and X. C. Wang, Dynamic effects of high-pressure pulsed water jet in low-permeability coal seams, *Journal of Coal Science and Engineering (China)*, 15 (3) (2009) 284-288.

[32] S. W. Rienstra, A small Strouhal number analysis for acoustic wave-jet flow-pipe interaction, *Journal of Sound and Vibration*, 86 (4) (1983) 539-556.

[33] J. Herrmann, J. Koreck, M. Maess, L. Gaul and O. V. Estorff, Frequency-dependent damping model for the hydroacoustic finite element analysis of fluid-filled pipes with diameter changes, *Mechanical Systems and Signal Processing*, 25 (3) (2011) 981-990.

[34] Y. Lu, X. Li and L. Yang, Effects of gas content in fluid on oscillating frequencies of self-excited oscillation water jets, *Journal of Fluids Engineering*, 126 (6) (2004) 1058-1061.

[35] R. C. Chanaud, Effects of geometry on the resonance frequency of Helmholtz resonators, *Journal of Sound and Vibration*, 178 (3) (1994) 337-348.

[36] S. Lai and Z. Liao, The Theory and Experimental Study of the Self-Excited Oscillation Pulsed Jet Nozzle (Pipeline Pulsed Flow Generator), *Natural Resources*, 4 (5) (2013) 395-403.

[37] D. Li, Y. Kang, X. Ding, X. Wang and Z. Fang, Effects of area discontinuity at nozzle inlet on the characteristics of high speed self-excited oscillation pulsed waterjets, *Experimental Thermal and Fluid Science*, 79 (2016) 254-265.

[38] D. Li, Y. Kang, X. Ding, X. Wang and Z. Fang, An experimental investigation on the pressure characteristics of high speed self-resonating pulsed waterjets influenced by feeding pipe diameter, *Journal of Mechanical Science and Technology*, 30 (11) (2016) 4997-5007.

Deng Li received his B.S. degree from Wuhan University, China, in 2012, and is now a Ph.D. candidate in School of Power and Mechanical Engineering, Wuhan University. He is currently a two-year visiting student at University of Illinois at Urbana-Champaign, United States.

Yong Kang received his B.S. and Ph.D. degrees from Chongqing University, China, in 2001 and 2006. He is now a Professor at School of Mechanical Engineering, Wuhan University, China.